

AD-A089 135

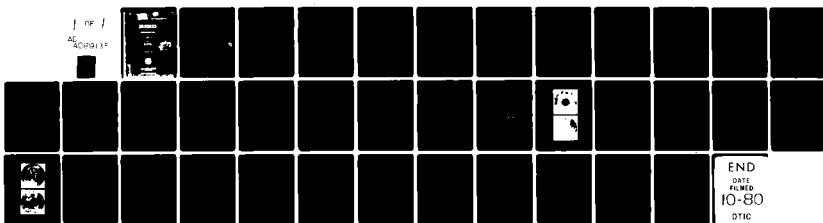
NAVAL RESEARCH LAB WASHINGTON DC
VECTOR-POTENTIAL FLOW IN RELATIVISTIC BEAM DIODES.(U)
SEP 80 D P BACON, S A GOLDSTEIN, R LEE

F/6 9/1

UNCLASSIFIED NRL-MR-4326

NL

1 OF 1
AL ADRISE



END
DATE
FILMED
10-80
DTIC

AD A089135

9 Memorandum rept.

SECURITY CLASSIFICATION OF THIS PAGE (When Data Entered)

REPORT DOCUMENTATION PAGE		READ INSTRUCTIONS BEFORE COMPLETING FORM	
1. REPORT NUMBER NRL-MR-4326	2. GOVT ACCESSION NO. AD-A089	3. RECIPIENT'S CATALOG NUMBER 135	
4. TITLE (and Subtitle) VECTOR-POTENTIAL FLOW IN RELATIVISTIC BEAM DIODES		5. TYPE OF REPORT & PERIOD COVERED Interim report on a continuing NRL problem.	
6. PERFORMING ORG. REPORT NUMBER		7. CONTRACT OR GRANT NUMBER(s)	
8. AUTHOR(s) D.P. Bacon, S.A. Goldstein, R. Lee, and G. Cooperstein		9. PERFORMING ORGANIZATION NAME AND ADDRESS Naval Research Laboratory Washington, D.C. 20375	
10. CONTROLLING OFFICE NAME AND ADDRESS Department of Energy Washington, D.C. 20545		11. PROGRAM ELEMENT, PROJECT, TASK AREA & WORK UNIT NUMBERS 67-0879-0-0	
12. MONITORING AGENCY NAME & ADDRESS (if different from Controlling Office) 12 138		13. REPORT DATE September, 1980	
		14. NUMBER OF PAGES 37	
		15. SECURITY CLASS. (of this report) UNCLASSIFIED	
		15a. DECLASSIFICATION/DOWNGRADING SCHEDULE	
16. DISTRIBUTION STATEMENT (of this Report) Approved for public release; distribution unlimited.			
17. DISTRIBUTION STATEMENT (of the abstract entered in Block 20, if different from Report)			
18. SUPPLEMENTARY NOTES †Present address: Dartmouth College, Department of Physics and Astronomy, Hanover, N.H. 03755 *Present address: JAYCOR, Alexandria, Virginia 22304			
19. KEY WORDS (Continue on reverse side if necessary and identify by block number) Intense relativistic electron beams High voltage diodes Para-vector-potential flow Anode plasma suppression			
20. ABSTRACT (Continue on reverse side if necessary and identify by block number) Analytic theory, numerical simulations and experiments indicate that a combination of a bias current pinch and an ion induced pinch may allow the efficient pinching of electron beams generated in large aspect ratio diodes. In the new diode geometry, electrons flow radially inward along vector-potential field lines which lie close to the anode. As these electrons do not touch the anode, there is no plasma formation and consequent loss of energy to accelerated ions. Entering a region close to the axis in which an anode plasma does exist, these electrons undergo an ion induced pinch to still smaller radii. Since the bulk of the flow occurs along vector-potential field lines, we have coined this new diode the Paravector-potential diode.			

DTIC
ELECTED
SEP 15 1980

251950

CONTENTS

I. INTRODUCTION	1
II. EXPERIMENTAL APPARATUS	6
III. OBSERVATIONS	8
IV. CONCLUSIONS	13
V. ACKNOWLEDGMENTS	13
REFERENCES	27

Accession For	
NTIS GRA&I	<input checked="checked" type="checkbox"/>
DDC TAB	<input type="checkbox"/>
Unannounced	<input type="checkbox"/>
Justification	
By _____	
Distribution/	
Availability Codes	
Dist	Avail and/or special
A	

VECTOR-POTENTIAL FLOW IN RELATIVISTIC BEAM DIODES

I. INTRODUCTION AND THEORY

Pinched electron flows in diodes have been used as a means of concentrating relativistic electron beam kinetic energy onto small areas. Inertial confinement fusion with relativistic electron beams has been a prime motivation for experimental and theoretical efforts directed at maximizing the electron power concentration. During recent studies it was found that hollow cathodes generate a collapsing hollow ring¹ that pinches because of an ion induced pinch.^{2,3} Prior to these discoveries, it was speculated that the electron flow pinches in vacuum^{4,5} due to the self-magnetic field generated by the electron flow current when it exceeded a critical current for pinching.⁶ It has been shown that the relativistic effects⁷ of unneutralized electron flows under self-magnetic fields do not generate a tightly pinched electron flow, but rather a weakly pinched one. The reason for this is that

$$|\underline{E}|_{\text{SELF}} > |\underline{B}|_{\text{SELF}} \quad (1)$$

and electrons do not $\underline{E} \times \underline{B}$ drift under such conditions. The models^{4,5} for vacuum pinching, however, can be made self-consistent by adding a mysterious current flowing on the diode axis. This current adds to the total magnetic field reversing inequality (1). The resulting electron flow is described by a force-free flow which has been coined^{4,5} Para-Potential Flow (PPF). One may then summarize the ion induced pinch and the PPF described above for generating pinched electron flow as two ways of reversing inequality (1). The ion induced pinch introduces ions that reduce the electric field while the PPF scheme

introduces a bias current that increases the magnetic field. The latter shall be called a bias current pinch since the PPF is only one of a family of electron flows that $\underline{E} \times \underline{B}$ drift towards the diode axis.

There is a definite advantage of bias current pinches over ion induced pinches for low impedance ($\leq 1 \Omega$) generators. The ion current that flows in low impedance pinched beam diodes restricts^{2,8} the electron power to a finite level ($\sim 10^{12}$ W) and is thus an unacceptable power drain for electron beam fusion (but is an interesting source of power for ion beams^{2,9}). Historically, there were many attempts to generate bias current pinches. These included the use of (1) tapered hollow cathodes¹⁰, (2) a plasma column on the diode axis,¹¹ (3) an externally driven rod on the diode axis,¹² (4) two concentric cathodes¹³ and recently (5) multiple cathodes.¹⁴

Here, we report on a new technique that is a combination of a bias current pinch and an ion induced pinch (Figure 1). This technique allows one either to minimize the ion current or to concentrate it near the axis. In addition, electron injection into the diode is radial rather than the axial emission of electrons from cathodes used to date. The radial injection was attempted as a smooth transition for electrons from the cathode to the equipotential surfaces (see the electron trajectories shown in Figure 1). Since electrons must cross equipotentials starting from the cathode (where the potential $\phi = 0$) on their way to motion along the equipotential surfaces near the anode, they cannot be characterized by a PPF theory. A more general theory which is restricted only to cold electron flow⁷ shows that the

mechanical momentum of the electron fluid is related to the magnetic field by

$$\vec{\nabla} \times \vec{P} = -\frac{e}{c} \vec{B} \quad (2)$$

Since $\vec{B} = \vec{\nabla} \times \vec{A}$, and A is free to be defined within the addition of any $\vec{\nabla}\chi$, one may realize

$$\vec{P} = -\frac{e}{c} \vec{A} \quad (3)$$

by choosing $\vec{\nabla}\chi = 0$. Thus the electron mechanical momentum vector lies along the vector potential. Hence the name Paravector-potential (PVP) diode.

The actual solutions of the electron flow for the geometry of Figure 1 near the inner edge of the outer cathode and the anode edge are rather complicated. The exact solutions at smaller radii will depend on an analytic continuation of the flow pattern from the regions of the corners into the smooth region of the flat anode. A family of solutions which are exact solutions of the generalized equation⁷ is given by a treatment similar to that of the reference.

The solutions are based on the existence of a region of zero electric field ((a) in Figure 1), an electron sheath of thickness d_1 (region (b)), and a vacuum region of thickness d_2 (region (c)). The magnetic field in region (a) is derived from the bias current of the center cathode, and ions flowing to it from the anode. Electrons from the outer cathode flow without being lost on the anode at radii

between the two cathodes. Using the forms of the electric and magnetic fields of the electron flow as derived by Goldstein, et al.,⁷ the thickness of the electron flow d_1 , and the thickness of the flow-anode vacuum gap. d_2 , are found as functions of radius.

$$d_1 = r \left(\frac{I_o}{I_c} \right) F \left(\frac{I_t}{I_c} \right) \quad (4)$$

$$d_2 = r \left(\frac{I_o}{I_c} \right) \left(\gamma_o - \frac{I_t}{I_c} \right) G \left(\frac{I_t}{I_c} \right) \quad (5)$$

Here r is the radius, $I_o = \frac{m_e c^3}{e} = 17 \text{ kA}$, I_c is the center current, $\gamma_o = 1 + \left| \frac{e V_o}{M_e c^2} \right|$, V_o the diode voltage, and the functions F and G are given by

$$F(x) = \frac{1}{2} \ln(x + (x^2 - 1)^{1/2}) \quad (6)$$

$$G(x) = \frac{1}{2} \left\{ \frac{x + (x^2 - 1)^{1/2}}{x^2 + x(x^2 - 1)^{1/2} - 1} \right\} \quad (7)$$

Over the range $2 \leq x \leq 3$, $F(x)$ and $G(x)$ are approximately 0.8 and 0.25, respectively.

It is important to note that for a given diode voltage, the gaps are totally defined by the ratio $\frac{I_t}{I_c}$. The physical anode-cathode spacing in region (a) does not enter into the result.

Since d_2 must be positive (or else the electrons will strike the anode), I_c must be greater than $\frac{1}{\gamma_o} I_t$. As d_2 is the distance between the flow and the anode, it provides a measure of the axial anode perturbations that the diode can tolerate. For example, for diode

parameters of 1 MV, 1 MA, and $\frac{I_t}{I_c} = 2.4$, the spacing $d_2 = (0.006)r$ while d_1 is a factor of 5 greater. Thus, at a radius of 4 cm, one can tolerate anode imperfections on the order of 0.02 cm.

If only electron flow existed, then the space charge effect of the flow from the outer cathode as it came opposite the inner cathode would have decreased the electron flow from the inner cathode, thus decreasing the bias current, resulting in the loss of the electrons on to the anode opposite the inner cathode. Taking into account that an anode plasma is being produced opposite the inner cathode by the electron beam heating of the anode surface, it is seen that ion flow may provide space-charge neutralization negating the effect of the radial electron flow and replacing the partially-suppressed electron current. The sum of the electron and ion currents in the center cathode represents the needed bias current. The presence of the ion flow allows an ion induced pinch to continue the pinching of the electron flow to radii smaller than the inner cathode. Numerical simulation^{15,16} has shown that, in this region, the drifts of electrons (such as the \vec{v}_B drift) are a prime cause for finite pinch radius. The use of smaller hole cathodes is known¹⁷ to generate smaller pinches and was also tried in the experiments reported here.

In the numerical simulation studies an extension of the r, z , semi-static, particle-in-cell code was used to find the self-consistent, numerical solutions of electron and ion flows. In Figure 2, the diode geometry and vacuum equipotentials are shown for diode parameters close to those used in the experiments. When self-consistent

particle flows are generated in this diode, the equipotential field lines (Figure 3) are drastically altered and shifted toward the anode in close agreement with analytic theory. The only constraint imposed was that ions on the anode were generated only at radii smaller than that of the inner cathode.

The basic concept of the PVP diode led to the design of a series of diodes used in conjunction with the GAMBLE I and GAMBLE II generators operated in positive polarity. The diode performance was studied over wide variations of voltage and total-to-center current ratio, I_t/I_c . In agreement with theory, it was found that given a total to inner current ratio less than γ_0 , then the radially injected electrons will flow inward without striking the anode at large radii providing there are no gaps or projections to perturb the equipotential surfaces. If the needed bias current is not provided, then a self-correcting phenomenon was observed in which excess radially injected electrons are lost immediately to the anode edge. The rest then flow in without striking the anode at large radii resulting in a current of $\gamma_0 I_c$ near the anode axis. The other predicted phenomenon observed was the interaction of the radial electron flow with the bias flow. Instead of continually rising during the voltage pulse, the bias current clamped at the value it had at the time the radial flow started.

II. EXPERIMENTAL APPARATUS

The PVP diode design has worked over the course of more than 80 shots. A scale drawing of the latest geometry is shown in Figure 4.

The cathodes (shown solid) were made from brass and mounted on a 36 cm diameter, 2.5 cm thick aluminum insert (shown cross-hatched) that fit the door of both of the GAMBLE relativistic beam generators, which were operated in positive polarity. The door insert had a 4.4 cm diameter hole on axis (originally 2.5 cm) and 1.0 cm slit 22.9 cm long cut through it (originally 19.7 cm) for viewing a diameter of the anode. The taper of the inner cathode was varied from 6° to 30° with a variety of inner and outer diameters. The most recent inner cathode was the 8.2/1.3 cm (O.D./I.C.), 12° tapered hollow cathode shown in Figure 4. The outer cathode was a 22.9 cm I.D., 25.4 O.D. brass ring. Shots using annular brass inserts to close the radial gap or tailor the emission surface have been taken. The anodes were originally flat aluminum disks (Figure 5a) 20 cm in diameter which were held onto the center conductor of GAMBLE I or GAMBLE II by 6 insulating bolts at a large radius. On later shots, the anode diameter was increased to close the radial gap. Spacers allowed the anodes to be positioned so as to be in the plane of the outer cathode. Later, in an attempt to reduce the edge damage, the outer edge was beveled at 45° (Figure 5b) to give the non-radially emitted electrons more distance in which to turn. Only in the last series of shots was the outer edge geometry changed to that shown in Figures 4 and 5c - the anode edge being relatively sharp and the anode beveled at negative 45° . In this configuration, the axial electric field was reduced with the result that most of the current flowed radially. The anode was a 20.3 cm diameter, stainless steel outer structure (shown with fine hatching)

which held an aluminum insert (shown with large hatching). The space behind the insert was present to prevent shock damage to the stainless holder and the hub of the generator. The stainless holder was mounted with a single $\frac{1}{4}$ " - 20 screw into the generator. The entire anode surface was covered with either 2 μ m aluminized KIMFOL polycarbonate foil or 6 μ m aluminized mylar, aluminum side towards the cathode. The covering provided the anode with a smooth, continuous potential surface.

The main diagnostics were a diode voltage monitor, \dot{B} loops monitoring the current flowing from the center cathode and also from the total cathode assembly, anode witness plate damage, and x-ray production monitored by a time-integrated x-ray pinhole camera and calibrated p-i-n diodes.

III. OBSERVATIONS

Series I - GAMBLE I shots #5828-5836

This series of shots used 20.0 cm diameter flat aluminum anodes mounted with six bolts at a diameter of 18.4 cm. The bolts were counterbored so as not to protrude out of the plane of the anode. An insert into the outer cathode made the radial gap 5 mm (See Figure 5e). The anode was varied from being inserted 0.5 mm into the plane of the outer cathode to being withdrawn 0.5 mm from it. The inner cathode was an 8.4/3.9 cm (O.D./I.D.), 6° tapered hollow cathode and the anode-cathode gap was 5.2 mm at the inner diameter.

The voltage on these shots was low (≤ 400 kV) and the bias current criterion was not met. Only 100 kA out of the 235 kA total current flowed in the center cathode which, according to the theory of PVP flow,

could bring in 80 kA from the outer cathode leaving 55 kA to strike the anode rim. Anode rims showed existence of radial flow through their extensive damage. The inner edges of the screw holes showed evidence that the beam had struck them on its way in lending support for the existence of radial flow.

The other conclusion from this series of experiments is that the very large area anode (314 cm^2) could not turn on an anode plasma during the 50 ns pulse time so that an ion induced pinch could not take place. This is in agreement with the areal velocity³ on aluminum ($\sim 2 \text{ cm}^2/\text{ns} \cdot 100 \text{ kA}$) which brought the collapsing hollow ring from a radius of 10 cm to a radius of 9 cm.

Series II - GAMBLE I Shots #5837 and 5845

For these shots, the same aluminum anodes were used as well as the same inner cathode. However, the outer cathode had finger stock mounted on its inner edge instead of an insert (Figure 5f). The inner cathode provided the required bias current and was nearly equal to $\frac{1}{\gamma_o} I_t$ for almost the total pulse time. The anodes showed little edge damage and had a rear-surface spall of 1.1 cm diameter on axis. The x-ray pinhole photograph for shot #5845 shows a 7 mm (FWHM) pinch. Figure 6 shows the front (top) and back of the anode for shot #5845. Note the slight damage at the inner edge of the screw holes. Figures 7 and 8 show the diode parameters for the same shot. It is significant to note that the outer cathode did not turn on for 10-20 ns after the start of the current pulse. When the outer cathode did turn on, the inner cathode current was clamped at its then current value and

remained nearly equal to $\frac{1}{Y} I_t$ for the rest of the pulse. The value at which the inner current clamped was a factor of two below its operating value when used without the outer cathode. This agrees with our theoretical expectations of the effect of the radial electron flow on the behavior of the inner cathode.

Series III - GAMBLE I Shots #5847-5851

These shots were identical to the shots in Series II with the addition of a TRW streak camera looking at the ions emitted from the anode. The ions struck the silvered side of an optically-thin slab of Pilot-B scintillator covering a diameter. The scintillator was viewed with the streak camera. The streak camera photographs showed that there were no ions emitted at large radii (compared to the outer radius of the inner cathode) although there were some ions coming from just outside the inner cathode.

Series IV GAMBLE I Shots #5861-5868

These shots had a 45° beveled outer cathode insert (Figure 5g) and a 20.3 cm or 20.6 cm diameter, 45° beveled anode (Figure 5c). The reduced radial gap meant that the voltage was again low and the required bias current not supplied. This geometry did not prove successful.

Series V - GAMBLE II Shots #1731-1735

For the first series of shots on the higher power GAMBLE II generator, 20.6 cm diameter, 45° beveled anodes (Figure 5c) and an outer cathode with finger stock mounted on its inner edge (Figure 5f) were used. On none of these shots was the $\frac{1}{Y_o} I_t$ bias current supplied

Nevertheless, shot #1735 appeared to be a relative success.

Figures 9 and 10 show the diode parameters for shot #1735. The diode operated at 750 kV, 900 kA with a flat, 0.8Ω impedance during the plateau of the voltage pulse. Two things should be noticed: The bias current required (350 kA) to vacuum pinch all of the outer current was never supplied, and there was no delay time between the start of the inner and outer currents. Even so, 400 kA out of an outer current of 650 kA should have vacuum pinched.

Figure 11 shows the front (top) and back of the anode plate for shot #1735. Although there was a great deal of damage to the anode edge due to the 250 kA of excess current, most of the anode outside of the inner cathode radius is relatively undamaged. Most of the apparent damage seen in Figure 11 is aluminum melted by the pinch and deposited on the anode surface. The x-ray pinhole photograph confirms this as it shows relatively little x-rays coming from the region between the anode edge and the inner cathode compared to x-rays from the anode edge. This provides additional support for our theoretical expectation that $\gamma_o I_c$ will pinch with the excess outer current sloughing off to the anode edge.

Series VI - GAMBLE II Shots #1745-1748

These shots were identical to the last series except that the outer cathode had no finger stock insert (Figure 5d) in order to open the radial gap, and the inner cathode was a 2.5 cm I.D., 2.9 cm O.D., 30° tapered, hollow cathode. The sharp-edged center cathode tended to either not supply very much current, or to short out. However, for

shot #1748, the biasing criteria was satisfied through the peak of the voltage pulse (1 MV) but was not satisfied during the voltage fall. Again, the x-ray photograph shows little radiation between the anode edge and the inner cathode.

Series VII - GAMBLE I shots #6431-6447

This last series of shots used the geometry shown in Figure 4, the design of which was based on considerations described earlier. The electrical characteristics and x-ray photographs showed that this new geometry almost always met the biasing criterion and that there were few or no x-rays from the anode edge. Also, this diode operated with a shot-to-shot reproducibility of 10% in current and voltage. Figures 12 and 13 are the averaged diode behavior for the five shots 6442-6446. As was typical of the earlier successful GAMBLE I shots, there is a 10-20 ns time delay between the start of the total current and the start of the outer current.

In order to study the ion current, the anode was modified by drilling a 1.3 cm diameter hole on axis and mounting a 2 cm diameter disk of 120 μ m polyethylene over the hole. The anode was recessed slightly over the central 2 cm so that the polyethylene disk would not protrude. The mylar anode covering was cut away to expose this disk. The result of activation measurements on this system indicates that ion current densities of approximately 4 kA/cm² flow in the 2.5 cm diameter hole of the center cathode. These preliminary results will be further investigated.

IV. CONCLUSIONS

A comparison of analytic theory, numerical simulation results, and experiments indicates that bias current pinching via paravector-potential flow may indeed be realized. Detailed geometries of diodes specifically designed to allow a smooth transition from a PVP flow at large radii to an ion induced pinch flow at small radii were studied. With careful optimization, it may be possible to create very efficient electron pinches from large aspect ratio diodes.

It has been shown that the PVP diode concept allows the multiplication of the total current of a single, tapered, hollow cathode by a factor of γ_0 without changing the geometry of the hollow cathode. In addition a fraction $(1 - 1/\gamma_0)$ of this current may be electron current independent of the diode aspect ratio or impedance. This contrasts with single, hollow cathodes which rely on ion induced pinching and contain a smaller fraction of their total current in electron current. The same diode may, however, operate with a bias current exceeding $\frac{1}{\gamma_0} I_t$ by allowing efficient ion production inside the center cathode. Preliminary results are encouraging and will be investigated further.

V. ACKNOWLEDGMENTS

The authors wish to thank Dr. A. E. Blaugrund for the ion streak measurement and E. Bellafiore, A. Robinson, and J. W. Snider for their expert assistance.

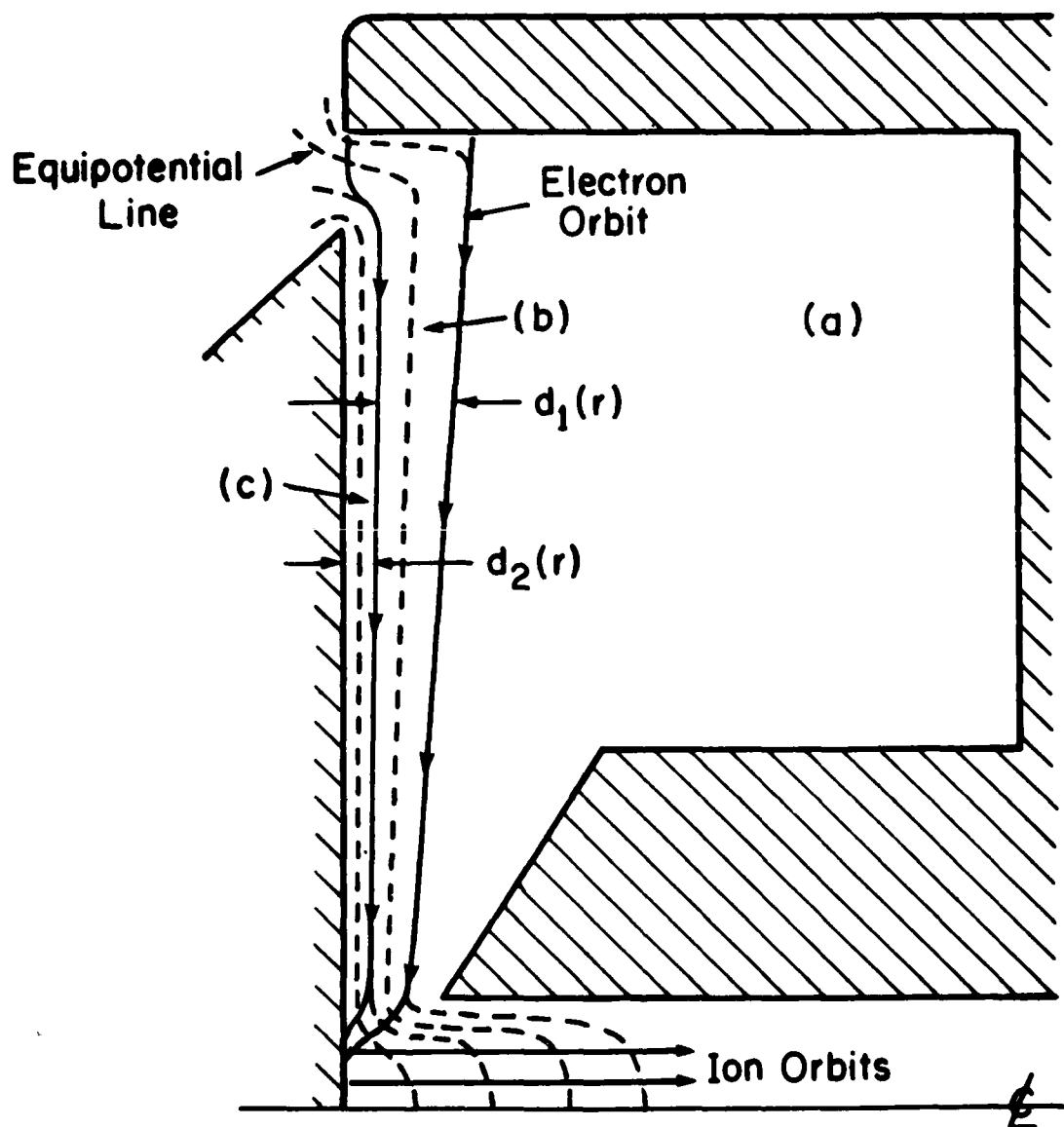


Fig. 1 — A conceptual drawing of the PVP diode.

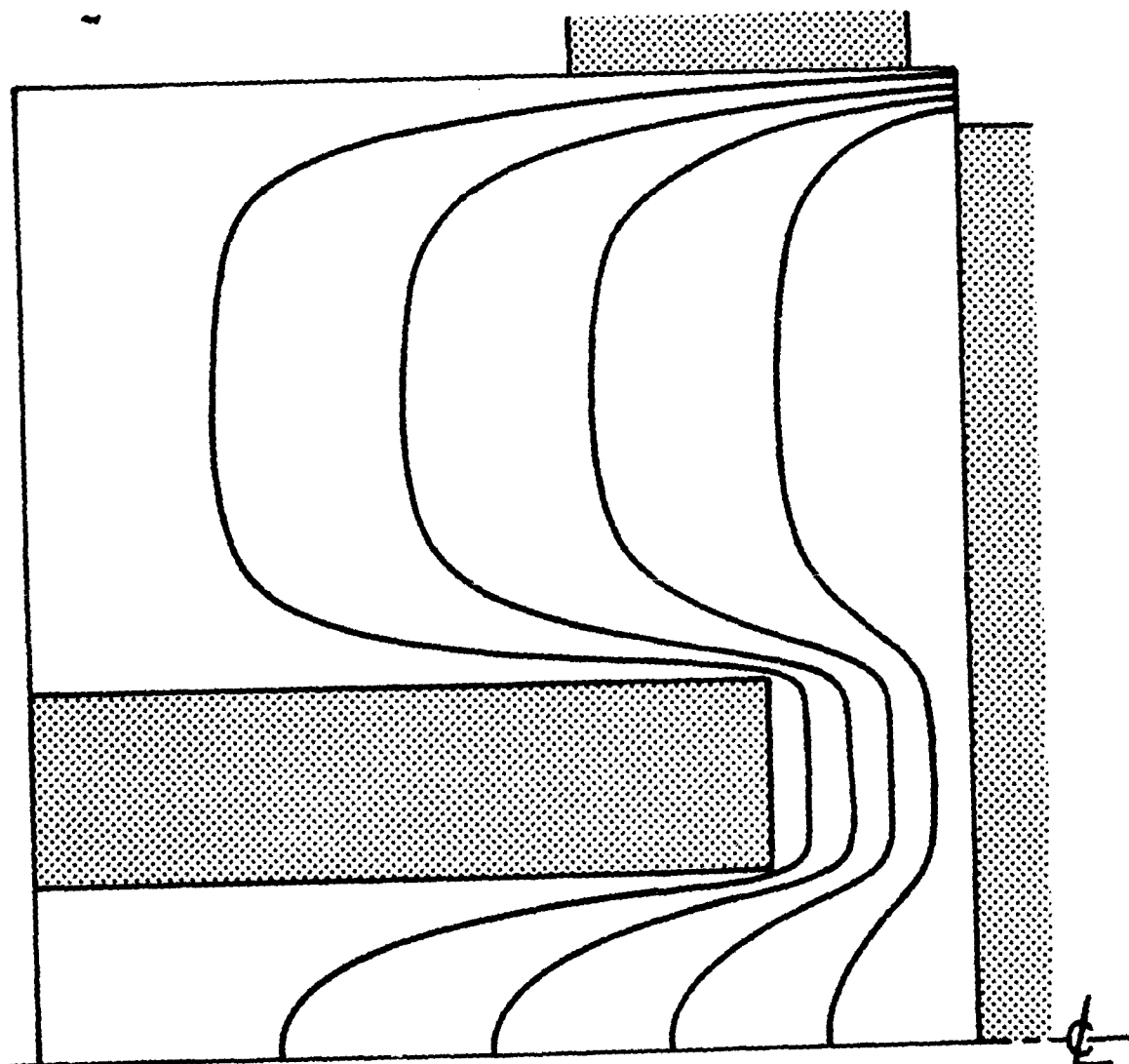


Fig. 2 — Numerical simulation of equipotential field lines prior to electrical emission.

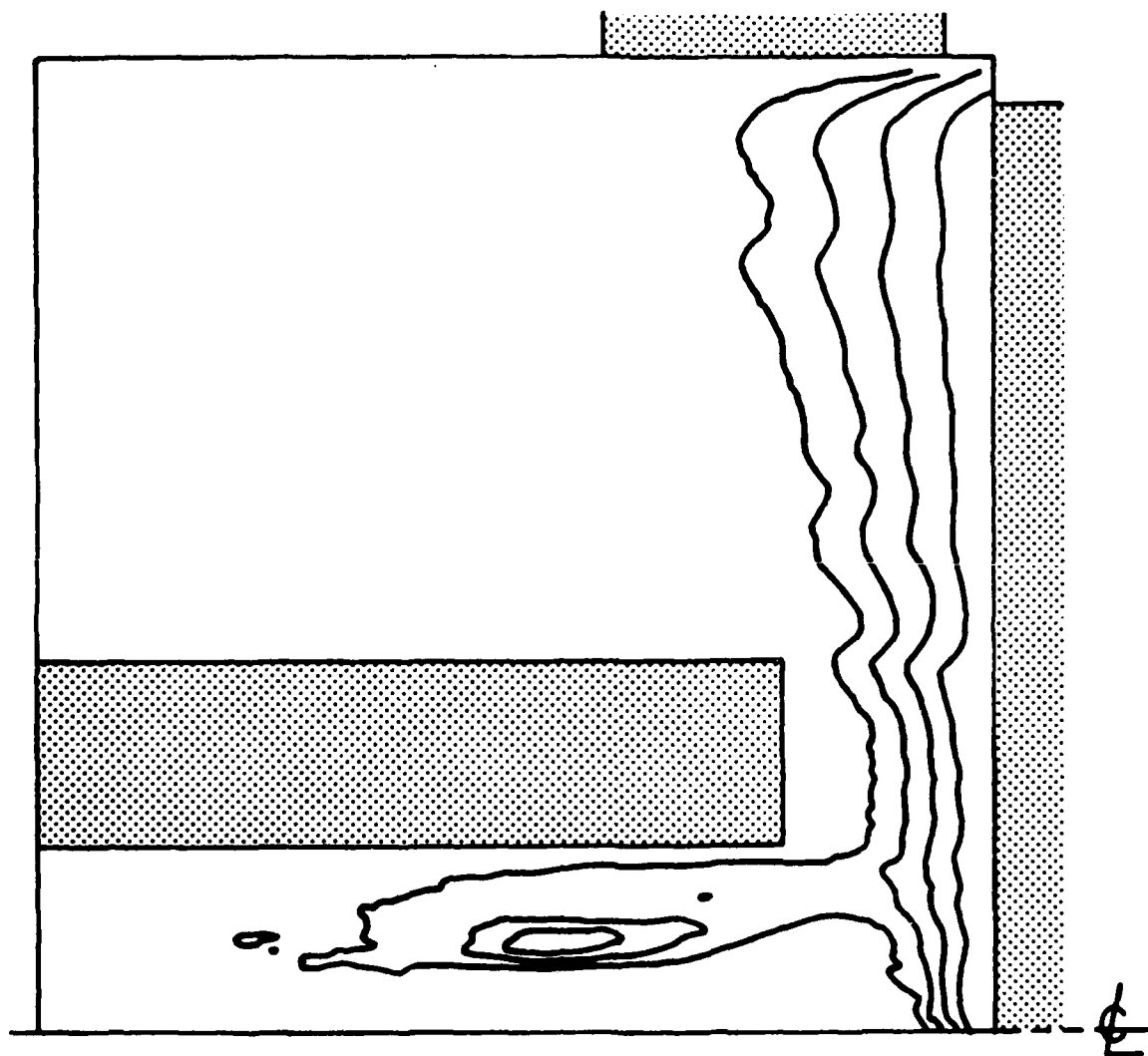


Fig. 3 — Numerical simulation of equipotential field lines after 2.5 ns of electron emission.

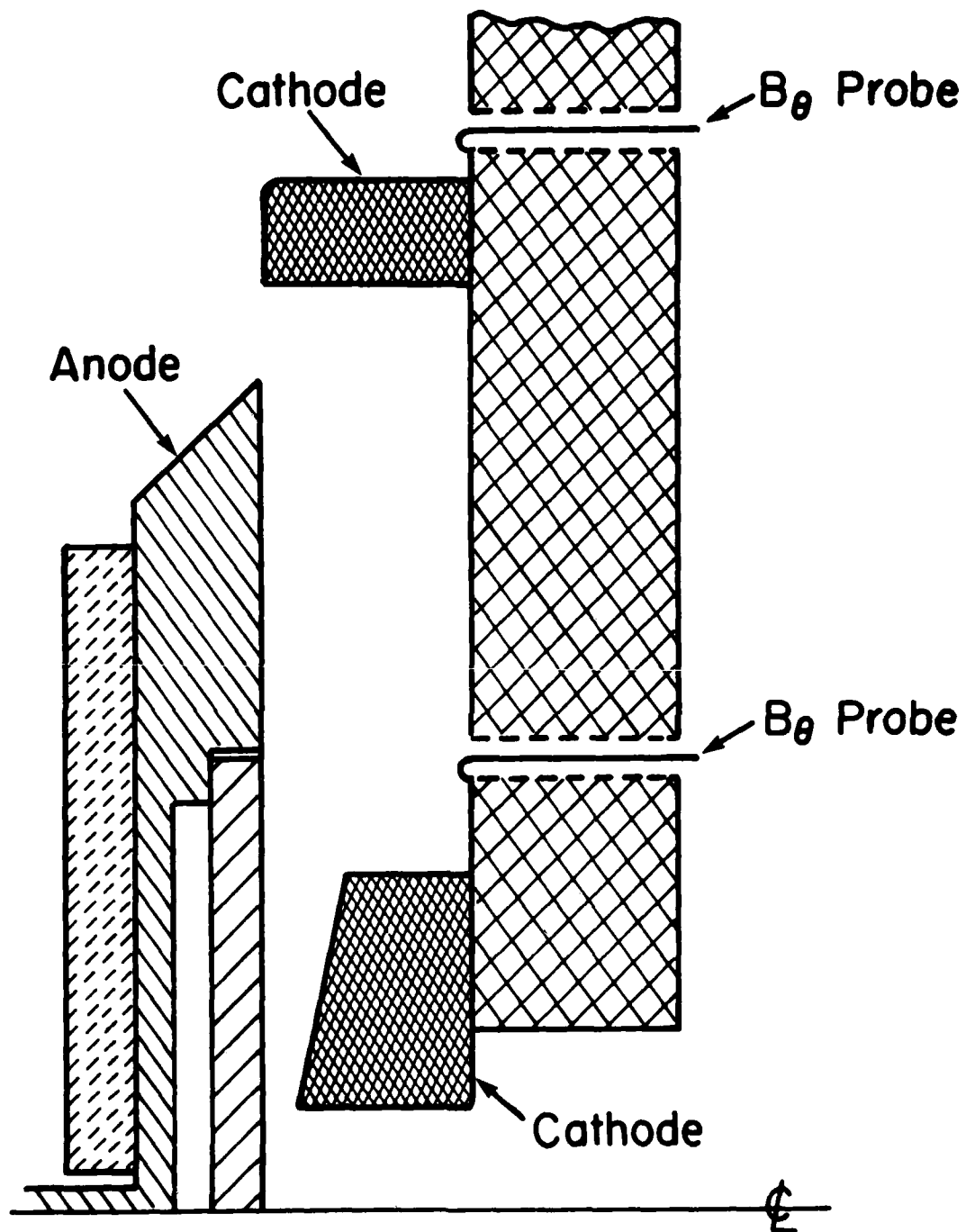
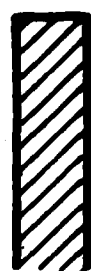
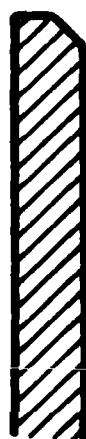


Fig. 4 — Scale drawing of latest PVP diode.



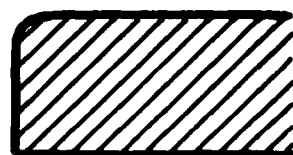
(a)



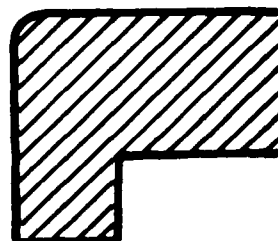
(b)



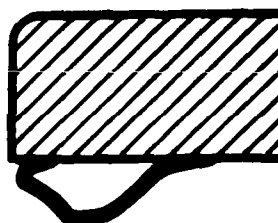
(c)



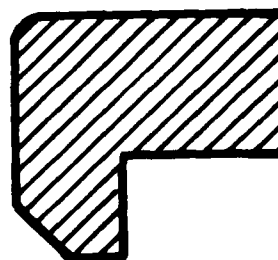
(d)



(e)



(f)



(g)

Anodes

Cathodes

Fig. 5 — Anode and outer cathode geometries used in these experiments.

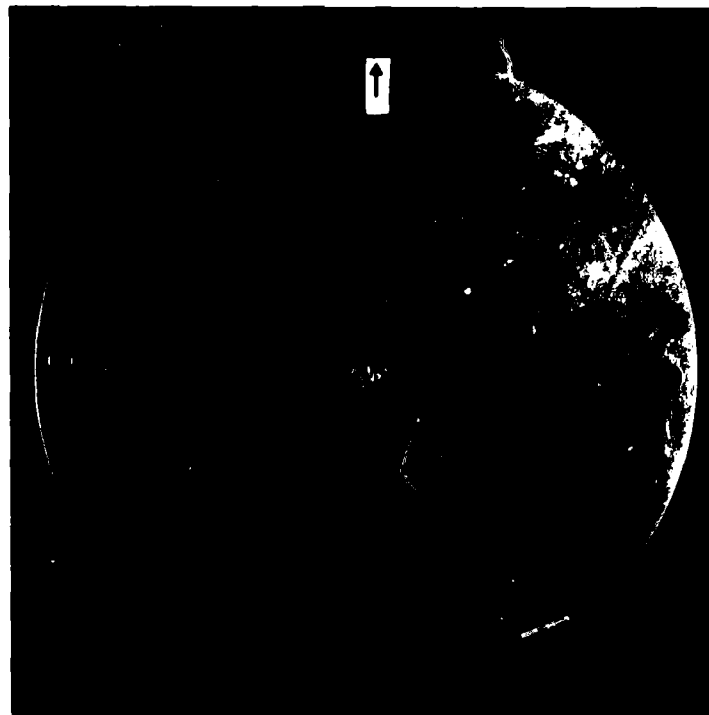
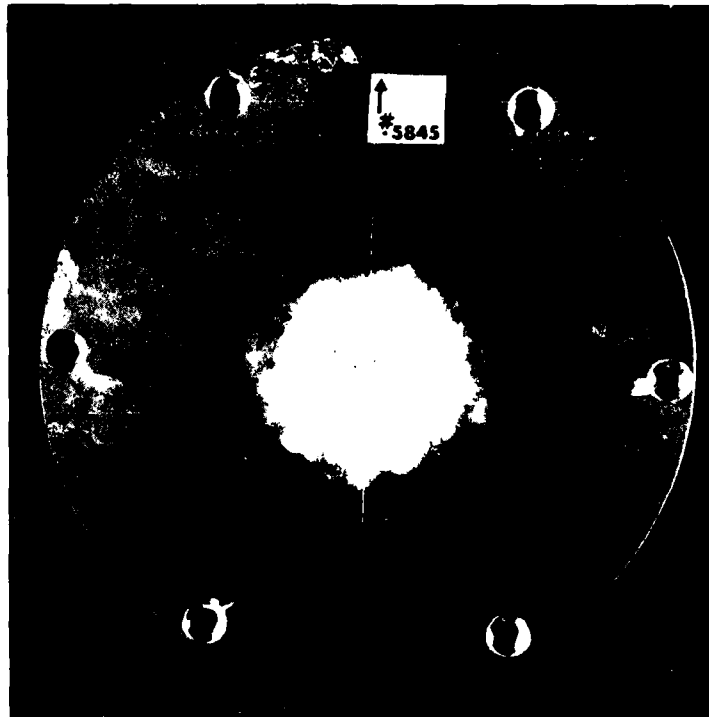


Fig. 6 Aluminum anode for shot #5845.

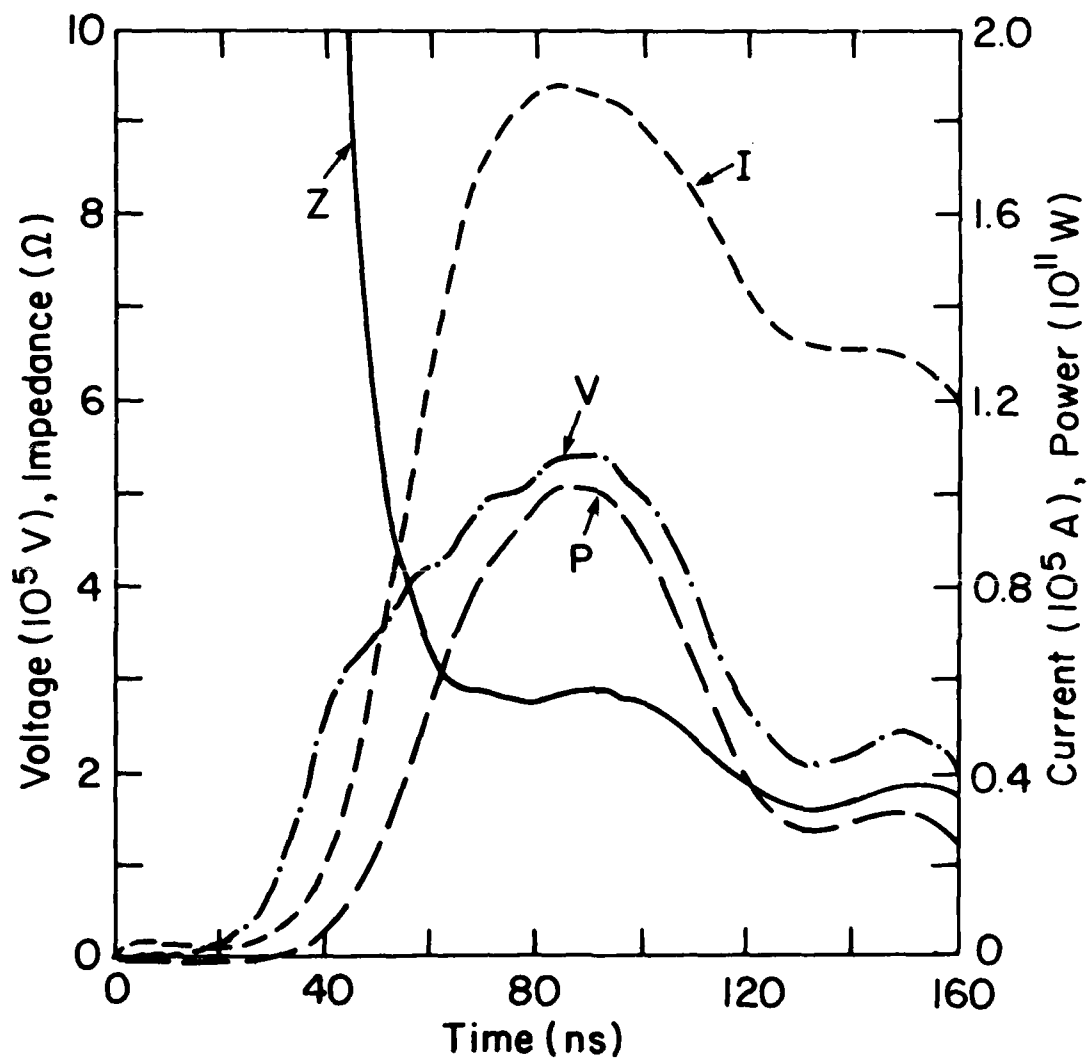


Fig. 7 — Overall diode parameters for shot #5845.

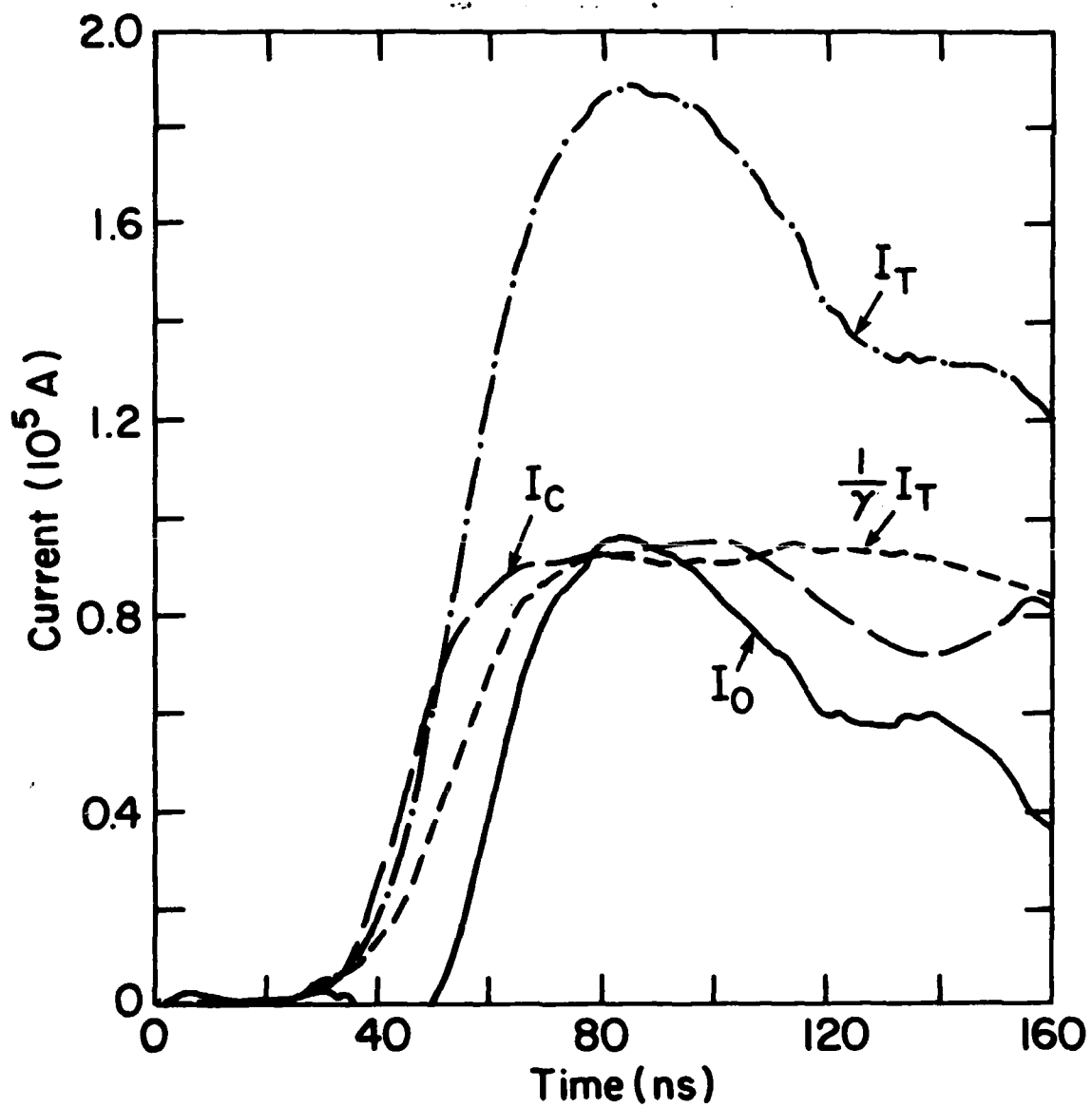


Fig. 8 — Inner, outer, total and theoretical bias current for shot #5845.

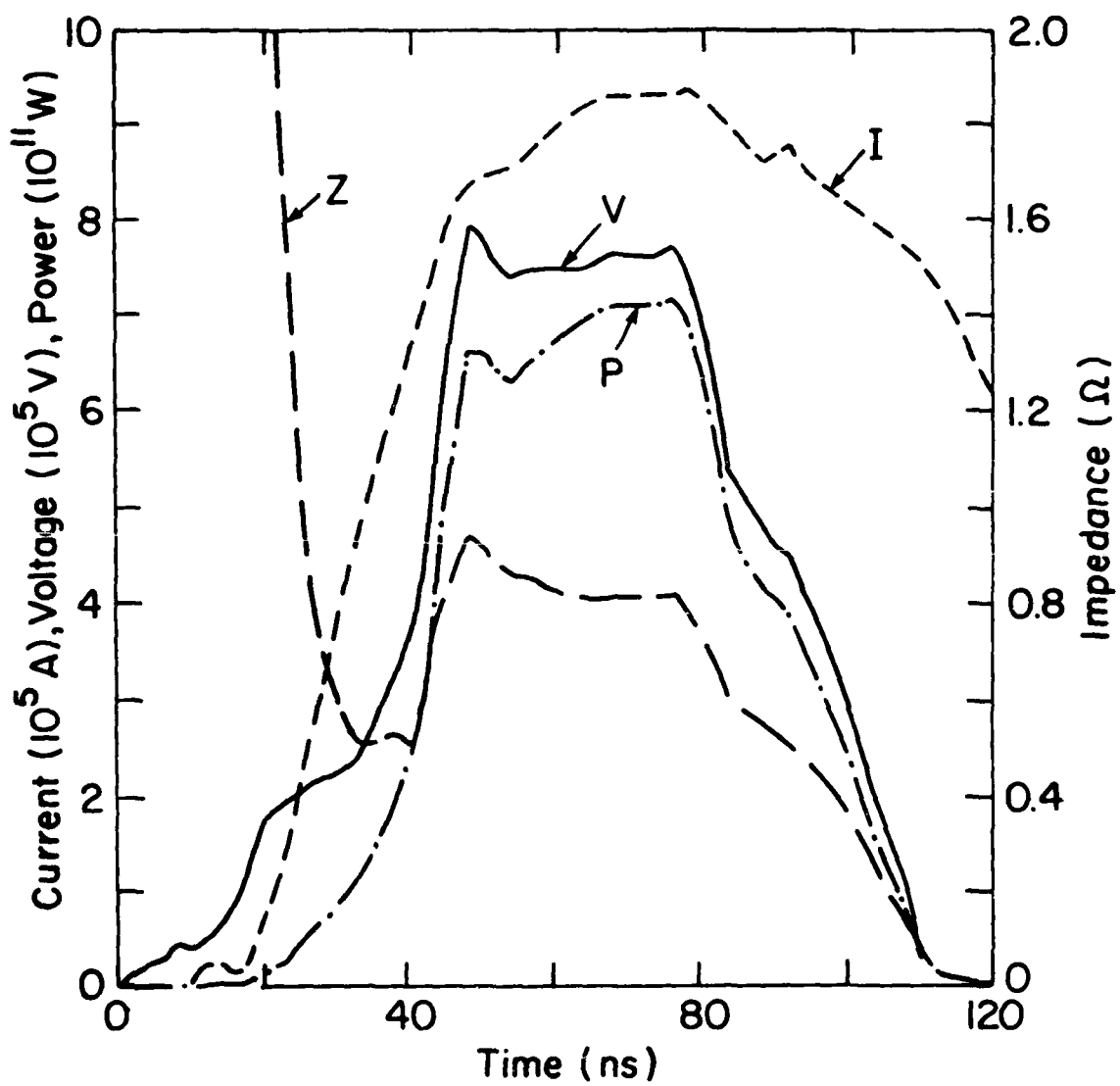


Fig. 9 — Overall diode parameters for shot #1735.

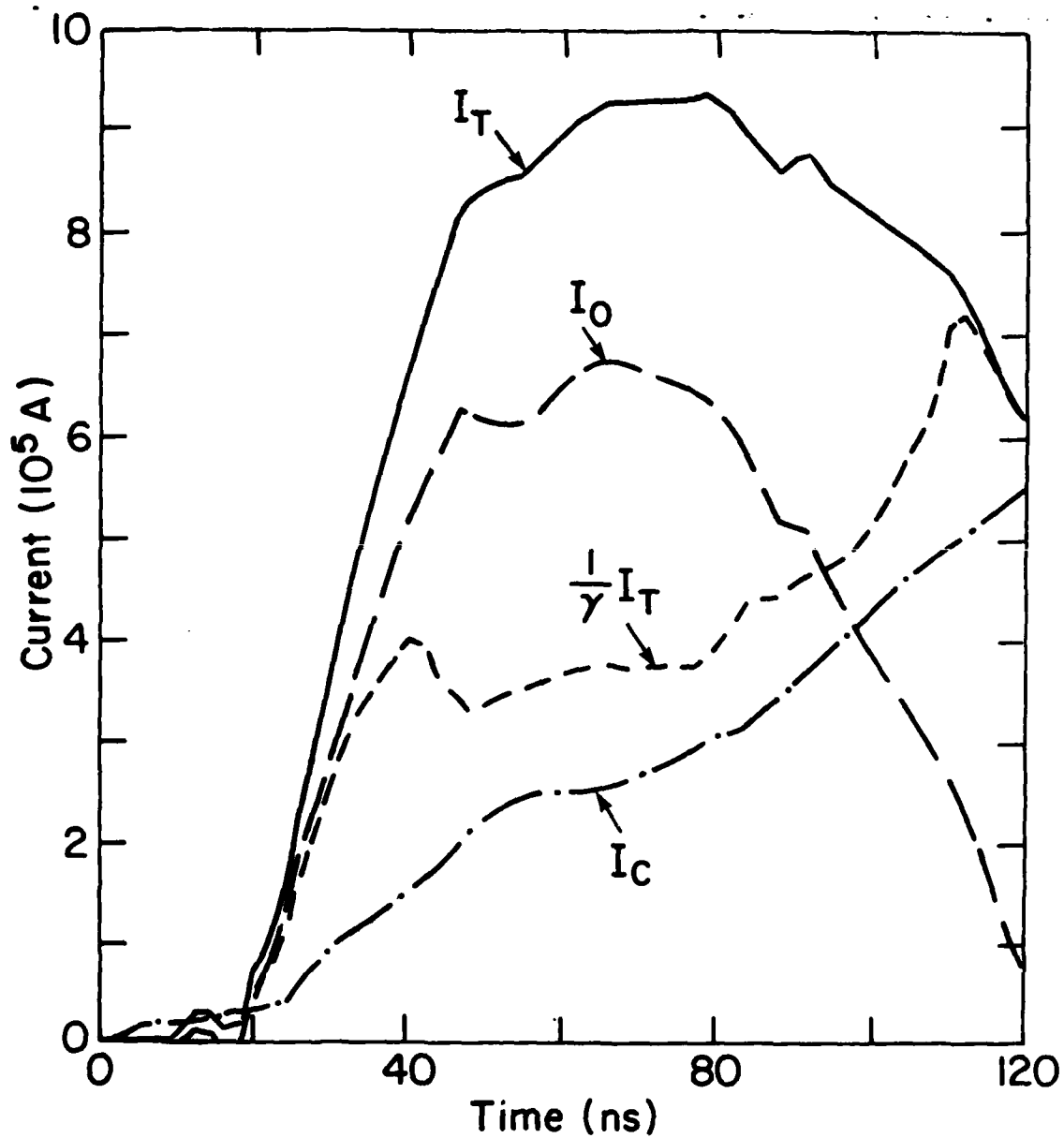


Fig. 10 — Inner, outer, total, and theoretical bias current for shot #1735.



Fig. 11 - Aluminum anode for shot #1735.

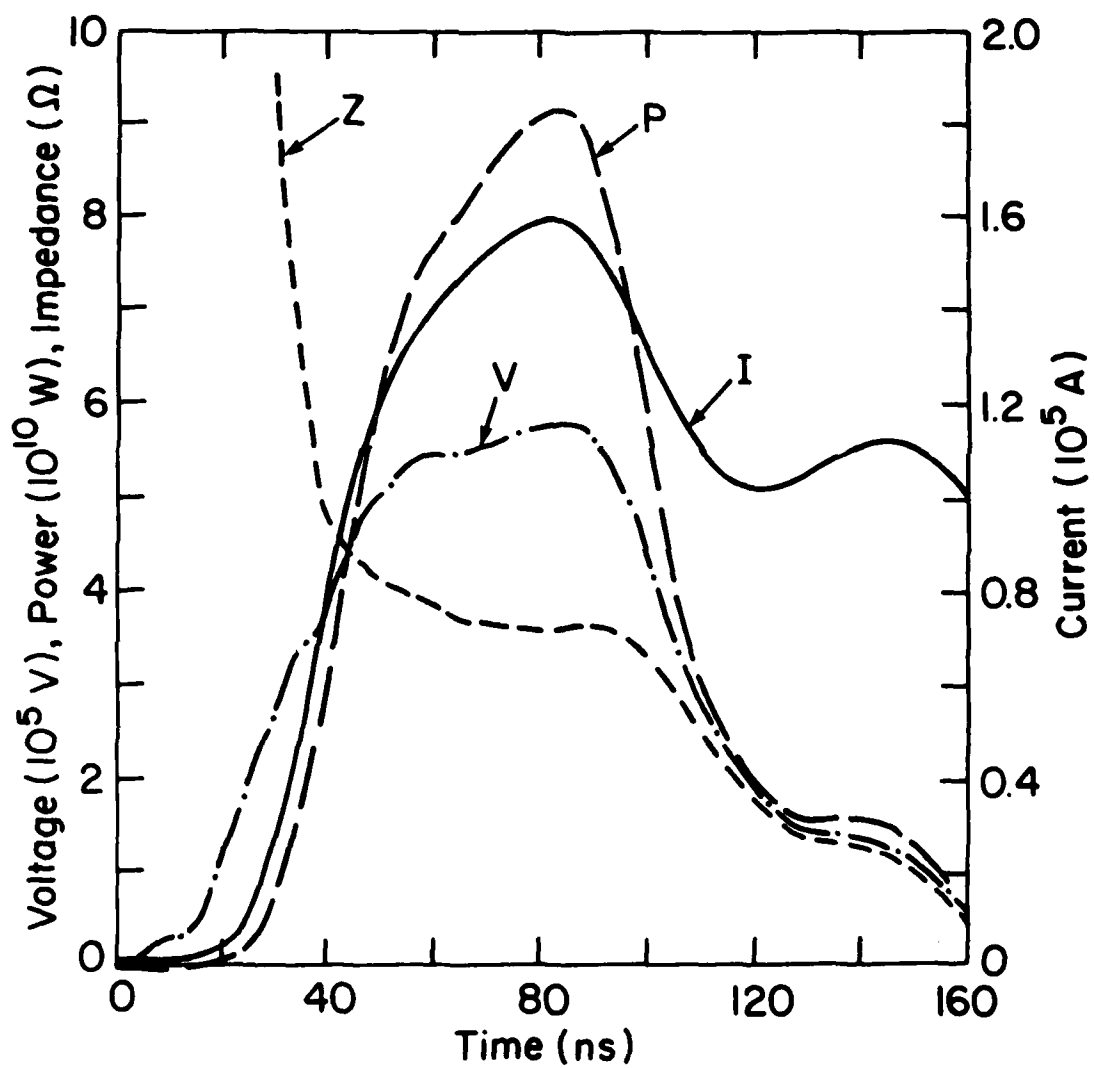


Fig. 12 — Average overall diode parameter for shots #6442-6446.

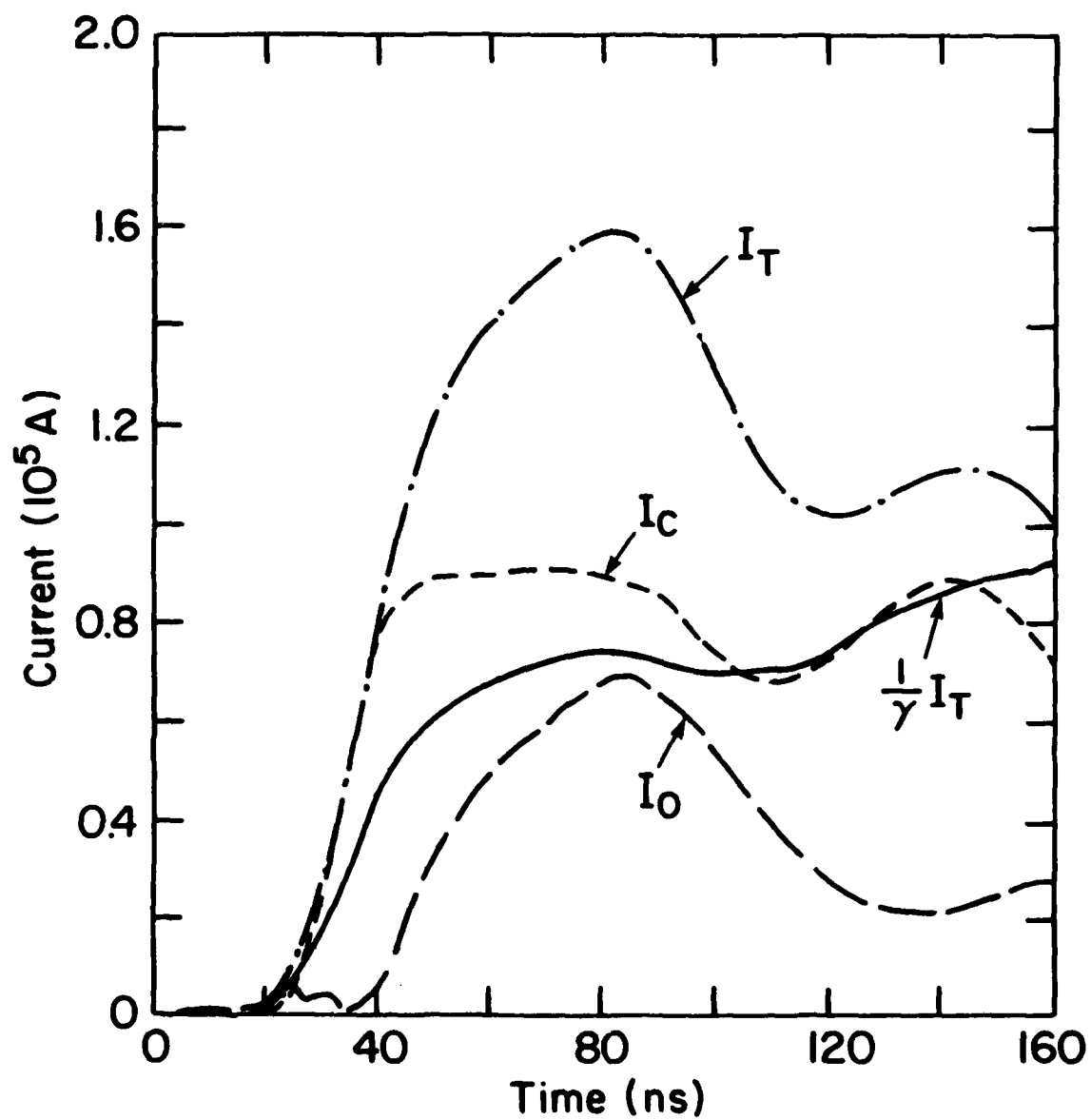


Fig. 13 — Average inner, outer, total, and theoretical bias current for shots #6442-6446.

REFERENCES

1. Blaugrund, A. E. and Cooperstein, G., Phys Rev Lett 34, 461 (1975).
2. Goldstein, Shyke A. and Lee, Roswell, Phys Rev Lett 35, 1979(1975).
3. Blaugrund, A. E., Cooperstein, G. and Goldstein, S. A., Phys of Fluids 20, 1185 (1977).
4. de Packh, D. and Ulrich, P. B., J. of Electronics and Control 10, 139 (1961), and de Packh, D., Naval Research Laboratory, Radiation Project Internal Report No. 5, 1968 (unpublished).
5. Creedon, J. M., J. Appl. Phys 46, 2946 (1975); and Phys Int'l Co. Report No. PIIR-17-72, 1972 (unpublished).
6. Friedlander, F., et al, Varian Associates Report No. DASA 2173, 1968 (unpublished).
7. Goldstein, S. A. et al, Phy Rev Lett 33, 1471 (1974).
8. Poukey, J. W., in Proc of the Int'l Topical Conf on Electron Beam Research and Technology, Albuquerque, NM, 1975, edited by Gerald Yonas (U. S. Dept. of Commerce, Washington, DC, (1976, p 247.
9. Stephanakis, S. J., et al, Phys Rev Lett 37, 1543 (1976).
10. de Packh, First experimental work on PPF cathodes on GI, (unpublished).
11. Yonas, G. et al, Phys Rev Lett. 30, 164 (1973).
12. Read, Michael, PhD Thesis, Cornell University (1976).
13. Cooperstein, G. in NRL Memorandum Report No. 3006, p. 60 (1975); and G. Yonas (private communication)
14. Mendel, C. W. and Goldstein, Steven (private communications).

15. Lee, Roswell, Goldstein, Shyke A. and Bacon, D. P., Bull. Am. Phys. Soc. 23, 762, (1978).
16. Quintenz, J. P., J. Appl. Phys. 49, 4377 (1978).
17. Johnson, D. J., et al, J. Appl. Phys. 49, 4634 (1978).

DISTRIBUTION LIST

Air Force Weapons Laboratory, AFSC
Kirtland AFB
Albuquerque, NM 87117

Attn: J. Darrah 1 copy

Argonne National Laboratory
9700 South Cass Avenue
Argonne, Illinois 60439

Attn: R. J. Martin 1 copy
G. R. Magelssen 1 copy

Brookhaven National Laboratory
Upton, NY 11973

Attn: A. F. Maschke 1 copy

Cornell University
Ithaca, NY 14850

Attn: R. N. Sudan 1 copy
D. A. Hammer 1 copy

Harry Diamond Laboratory
Aldelphi, MD 20733

Attn: S. Graybill 1 copy

Director
Defense Nuclear Agency
Washington, DC 20305

Attn: R. L. Gullickson (RAEV) 1 copy
J. Z. Farber (RAEV) 1 copy

Defense Technical Information Center
Cameron Station
5010 Duke Street
Alexandria, VA 22314

12 copies

Grumman Aerospace Corporation
Bethpage, NY 11714

Attn: P. Suh

1 copy

JAYCOR, Inc.
205 S. Whiting Street
Alexandria, VA 22304

Attn: D. A. Tidman
R. Hubbard
J. Guillory

1 copy
1 copy
1 copy

JAYCOR, Inc.
1401 Camino Del Mar
Del Mar, CA 92014

Attn: E. Wenaas

1 copy

JAYCOR, INC.
300 Unicorn Park Drive
Woburn, MA 01801

Attn: H. Linnestad

1 copy

Lawrence Livermore Laboratory
P. O. Box 808
Livermore, CA 94550

Attn: R. J. Briggs
R. O. Bangerter
J. H. Nuckolls
S. S. Yu
E. P. Lee

1 copy
1 copy
1 copy
1 copy
1 copy

Los Alamos Scientific Laboratory
P. O. Box 1663
Los Alamos, NM 87545

Attn: R. B. Perkins
L. E. Thode
D. B. Henderson

1 copy
1 copy
1 copy

Maxwell Laboratories, Inc.
9244 Balboa Avenue
San Diego, CA 92123

Attn: A. C. Kolb	1 copy
P. Korn	1 copy
J. Pearlman	1 copy
R. W. Clark	1 copy

Mission Research Corporation
735 State Street
Santa Barbara, CA 93101

Attn: C. L. Longmire	1 copy
----------------------	--------

Mission Research Corporation
1400 San Mateo Blvd. SE
Albuquerque, NM 87108

Attn: B. B. Godfrey	1 copy
---------------------	--------

National Bureau of Standards
Washington, DC 20234

Attn: J. Leiss	1 copy
----------------	--------

National Technical Information Service
U. S. Department of Commerce
5285 Port Royal Road
Springfield, VA 22161

24 copies

National Science Foundation
Mail Stop 19
Washington, DC 20550

Attn: D. Berley	1 copy
-----------------	--------

Naval Research Laboratory
Attn: Name/Code
Washington, DC 20375

Addressee:

Code 2628 - TIC-Distribution	25 copies
Code 6020 - J. Boris	1 copy
Code 6682 - D. Nagle	1 copy
Code 4700 - T. Coffey	25 copies
Code 4707 - J. Davis	1 copy
Code 4730 - S. Bodner	1 copy
Code 4740 - V. Granatstein	1 copy
Code 4760 - B. Robson	1 copy
Code 4761 - C. Kapetanakis	1 copy
Code 4770 - Branch Head	1 copy

Naval Research Laboratory (continued)
Attn: Name/Code
Washington, DC 20375

Addressee:

Code 4771 - D. Mosher	10 copies
Code 4773 - G. Cooperstein	10 copies
Code 4770 - I. Vitkovitsky	10 copies
Code 4790 - M. Lampe	1 copy
Code 4790 - I. Haber	1 copy
Code 4790 - D. Colombant	1 copy

Physics International Co.
2700 Merced Street
San Leandro, CA 94577

Attn: S. J. Putnam	1 copy
A. J. Toepfer	1 copy
P. W. Spence	1 copy
J. Benford	1 copy
R. Genuario	1 copy
J. Maenchen	1 copy
B. Bernstein	1 copy
E. B. Goldman	1 copy

R & D Associates
P. O. Box 9695
Marina Del Rey, CA 90291

Attn: L. Martineili	1 copy
M. Crover	1 copy

Sandia Laboratories
P. O. Box 5800
Albuquerque, NM 87115

Attn: G. Yonas	1 copy
G. W. Kuswa	1 copy
J. R. Freeman	1 copy
D. J. Johnson	1 copy
P. S. Miller	1 copy
J. P. Vandevender	1 copy
S. Humphries	1 copy

Stanford University
SLAC
P. O. Box 4349
Stanford, CA 94305

Attn: W. B. Herrmannsfeldt	1 copy
----------------------------	--------

Systems, Science and Software
P. O. Box 1620
La Jolla, CA 92038

Attn: A. Wilson

1 copy

University of California
Lawrence Livermore Laboratory
Berkeley, Ca 94720

Attn: D. Keefe

1 copy

University of California
Irvine, CA 92664

Attn: G. Benford
N. Rostoker

1 copy

1 copy

U. S. Department of Energy
P. O. Box 62
Oak Ridge, TN 37830

50 copies

U. S. Department of Energy
Division of Inertial Fusion
Washington, DC 20545

Attn: G. Canavan
T. F. Godlove

2 copies

1 copy

University of Illinois
Urbana, IL 61801

Attn: G. H. Miley
J. T. Verdeyen

1 copy

1 copy

University of Rochester
Laboratory of Laser Energetics
River Station, Hopeman 110
Rochester, NY 14627

Attn: M. J. Lubin

1 copy

Bhabha Atomic Research Centre
Bombay - 400085, India

Attn: B. K. Godwal 1 copy
A. S. Patthankar 1 copy

CEA, Centre de Etudes de Lemeil
B. P. 27
94120 Villeneuve, Saint George
France

Attn: A. Bernard 1 copy
A. Jolas 1 copy

CEA, Centre de Etudes de Valduc
P. B. 14
21120 Is-sur-Tille
France

Attn: C. Patou 1 copy
C. Peugeot 1 copy
M. Roche 1 copy
N. Camarcat 1 copy
C. Bruno 1 copy
J. Barbaro 1 copy

Ecole Polytechnique
Labo. PMI
91128 Palaiseau Cedex
France

Attn: H. Doucet 1 copy
J. M. Buzzi 1 copy

Institute of Laser Engineering
Osaka University
Yamadakami
Suita
Osaka 565, Japan

Attn: S. Nakai 1 copy
K. Imasaki 1 copy

Institut d'Electronique Fondamentale
Universite' Paris XI-Bat. 220
F91405 Orsay
France

Attn: G. Gautherin 1 copy

Institut Fur Neutronenphysik
un Reaktortechnik
Postfach 3640
Kernforschungszentrum
D-7500 Karlsruhe 1
West Germany

Attn: H. N. Karow 1 copy
W. Schmidt 1 copy

Instituto De Investigaciones Cientificas Y Technicas
De Las Fuerzas Armadas
Aufriategui y Varela
V. Martelli 1603
Pcia Bs. As. - R. Argentina

Attn: N. B. Camusso 1 copy

Institute of Atomic Energy
Academia Sinica - Peking
People's Republic of China

Attn: R. Hong 1 copy

Max-Planck-Institut fur Plasmaphysik
8046 Garching bei Munchen
West Germany

Attn: R. Lengyel 1 copy

Physical Research Laboratory
Navrangpura
Ahmedabad- 380009- India

Attn: V. Ramani 1 copy

Shivaji University
Kolhapur, India

Attn: L. N. Katkan 1 copy

Weizmann Institute of Science
Rehovot, Israel

Attn: A. E. Blaugrund 1 copy
Z. Zilmanon 1 copy
E. Nardi 1 copy

DATE
FILMED
0-8